First-principles study of correlation effects in VO_2

R. Sakuma,[1,2,3,*] T. Miyake,[1,2] and F. Aryasetiawan[1,2,3]

[1]*Research Institute for Computational Sciences, National Institute of Advanced Industrial Science and Technology, Tsukuba, Ibaraki 305-8568, Japan*

[2]*CREST, Japan Science and Technology Agency, Kawaguchi, Saitama 332-0012, Japan*

[3]*Graduate School of Advanced Integration Science, Chiba University, Chiba 263-8522, Japan*

(Received 7 April 2008; published 8 August 2008)

We present a first-principles study of VO_2 in the rutile and monoclinic (M_1) phases by means of all-electron full-potential linear muffin-tin orbital GW calculation. Full frequency dependence and off-diagonal matrix elements of the self-energy are taken into account. As a result of dynamical correlations, a satellite structure is found above the t_{2g} quasiparticle peak, although not below, in both the rutile and monoclinic phases. For the monoclinic structure, the insulating state is not obtained within the usual one-shot GW calculation. We have performed a simplified "self-consistent" GW scheme by adding a uniform shift to the conduction-band levels and recalculating the quasiparticle wave functions accordingly. An insulating solution with a gap of approximately 0.6 eV is obtained, in agreement with experiments.

DOI: 10.1103/PhysRevB.78.075106 PACS number(s): 71.30.+h, 71.20.Be

I. INTRODUCTION

Vanadium dioxide undergoes a metal-insulator transition (MIT) at the transition temperature $\approx$340 K.[1] Much work has been done both experimentally and theoretically to investigate the role of electron correlations in this transition. At high temperature VO_2 is metallic and forms a tetragonal rutile (R) structure with space-group $P4_2/mnm$ while at low temperature, it forms a monoclinic (M_1) structure with space-group $P2_1/c$ and becomes insulating with a band gap of 0.6 eV.[2] A striking feature of the M_1 phase is the dimerization of vanadium atoms with the zigzaglike displacements, which leads to a doubling of the unit cell along the c axis. In both phases the crystal field splits vanadium t_{2g} bands into a doubly degenerate e_g^π band and a nondegenerate a_{1g} band. More than three decades ago, Goodenough[3] proposed a Peierls (bandlike) picture of the insulating state: in the metallic VO_2, the a_{1g} band overlaps with the e_g^π band and both bands are partially filled. In the insulating VO_2, the pairing of vanadium atoms leads to the bonding-antibonding splitting of two a_{1g} bands, and separates the bonding a_{1g} band and e_g^π band. The bonding a_{1g} band becomes filled while the e_g^π band becomes empty and the gap opens up between them. This scenario is also supported by Wentzcovitch *et al.*,[4] who showed that first-principles molecular-dynamics calculations within the local-density approximation (LDA) of density-functional theory could reproduce the structure and energy difference of these two phases with good accuracy. They failed to reproduce the insulating monoclinic VO_2 and attributed this failure to the problem of the LDA. However, since this Peierls model cannot explain the metastable insulating state of another monoclinic (M_2) structure[5,6] where only half of the vanadium atoms are dimerized, the importance of electron-electron correlations has been emphasized.[7,8] To study the effects of correlations beyond the LDA, theoretical works using LDA+DMFT (dynamical mean-field theory[9]) have recently been done.[10–12] Liebsch *et al.*[10] performed a single-site multiband DMFT calculation with the quantum Monte Carlo method but their LDA+DMFT result did not reproduce an insulating VO_2. On the other hand, Laad *et al.*[11] concluded from their LDA+DMFT calculation within the iterative perturbation theory (IPT) that the MIT was of the Mott-Hubbard type. To account for the spatial correlation between dimerized vanadium atoms, Biermann *et al.*[12] performed cluster-DMFT calculations in this system and succeeded in reproducing the two phases. In their result for the insulating VO_2, the antibonding a_{1g} band is strongly renormalized to form the upper Hubbard band due to correlation. However, the peak of the spectral function just below the Fermi energy is, interestingly, not an incoherent lower Hubbard band but a quasiparticle peak of the a_{1g} band, which indicates that the insulating VO_2 has also a bandlike nature.

The above DMFT model approaches are parameter dependent and only a few bands are taken into account. Hence, a first-principles description without adjustable parameters is highly desirable. The GW approximation (GWA) (Refs. 13 and 14) has been successfully applied to calculations of excited-state properties of a wide range of materials; thus the GWA may be appropriate for this problem. However, due to the system size of VO_2 (monoclinic VO_2 has 12 atoms in a unit cell), a direct application of the GW method to this system has been limited. Continenza *et al.*[15] applied a simple model GW scheme to insulating VO_2 and succeeded in reproducing the band gap. In their approach, the self-energy was approximated by a *static* nonlocal potential in which the experimental value of the dielectric constant was used. Very recently Gatti *et al.*[16] performed a quasiparticle calculation with a simplified self-consistent GW scheme; they first carried out a self-consistent calculation within Hedin's Coulomb hole and screened exchange (COHSEX) approximation,[13] and used the resulting self-consistent one-particle wave functions and energies as an input for a one-shot GW calculation. Using this procedure they also obtained a band gap, in good agreement with experiment.

In the present work, we also perform GW calculations in order to gain better understanding of electron correlation effects in VO_2 with special emphasis on the influence of the diagonal self-energy and the role of dynamical effect in the

self-energy, going beyond a model or static treatment of the self-energy. We find that the self-energy is in fact strongly energy dependent and it affects significantly the one-electron excitation spectrum. We also find that the off-diagonal self-energy can have a large influence on the quasiparticle band structure. Our calculations reproduce both the metallic and insulating VO_2.

II. METHOD

In the GW method,[13,14] the self-energy Σ is written as a product of one-particle Green's function G and the screened Coulomb interaction W:

$$\Sigma(\mathbf{r},\mathbf{r}',\omega) = \frac{i}{2\pi}\int G(\mathbf{r},\mathbf{r}',\omega+\omega')W(\mathbf{r},\mathbf{r}',\omega')d\omega'. \quad (1)$$

Here W is calculated within the random-phase approximation (RPA). The quasiparticle wave functions $\{f_{\mathbf{k}\nu}\}$ and energies $\{\varepsilon^{\mathrm{GW}}_{\mathbf{k}\nu}\}$ satisfy the following equation:

$$\left[-\frac{1}{2}\nabla^2 + v_{\mathrm{ext}}(\mathbf{r}) + v_H(\mathbf{r})\right]f_{\mathbf{k}\nu}(\mathbf{r}) + \int \Sigma(\mathbf{r},\mathbf{r}',\varepsilon^{\mathrm{GW}}_{\mathbf{k}\nu})f_{\mathbf{k}\nu}(\mathbf{r}')d^3r' = \varepsilon^{\mathrm{GW}}_{\mathbf{k}\nu}f_{\mathbf{k}\nu}(\mathbf{r}), \quad (2)$$

where v_{ext} and v_H are the external and Hartree potential, respectively. Usually Eq. (2) is solved in a non-self-consistent way with two further approximations: first, the self-energy correction from the LDA exchange-correlation potential v^{LDA}_{xc} is assumed to be diagonal with respect to the LDA wave functions, $\Delta\Sigma_{\mu\nu}(\mathbf{k},\omega) = \langle\psi^{\mathrm{LDA}}_{\mathbf{k}\mu}|\hat{\Sigma}(\omega) - \hat{v}^{\mathrm{LDA}}_{xc}|\psi^{\mathrm{LDA}}_{\mathbf{k}\nu}\rangle = \delta_{\mu\nu}\Delta\Sigma_{\nu\nu}(\mathbf{k},\omega)$. Second, the frequency dependence of the self-energy is simplified by the linearization around the LDA eigenenergies,

$$\Sigma_{\nu\nu}(\mathbf{k},\omega) \approx \Sigma_{\nu\nu}(\mathbf{k},\varepsilon^{\mathrm{LDA}}_{\mathbf{k}\nu}) + \left.\frac{\partial\Sigma_{\nu\nu}}{\partial\omega}\right|_{\omega=\varepsilon^{\mathrm{LDA}}_{\mathbf{k}\nu}}(\omega-\varepsilon^{\mathrm{LDA}}_{\mathbf{k}\nu}). \quad (3)$$

The quasiparticle energies are then evaluated as the first-order correction to the Kohn-Sham eigenvalues,

$$\varepsilon^{\mathrm{GW}}_{\mathbf{k}\nu} = \varepsilon^{\mathrm{LDA}}_{\mathbf{k}\nu} + Z_{\mathbf{k}\nu}\Delta\Sigma_{\nu\nu}(\mathbf{k},\varepsilon^{\mathrm{LDA}}_{\mathbf{k}\nu}), \quad (4)$$

where $Z_{\mathbf{k}\nu} = 1 - \left.\frac{\partial\Sigma_{\nu\nu}(\omega)}{\partial\omega}\right|_{\omega=\varepsilon^{\mathrm{LDA}}_{\mathbf{k}\nu}}$ is the renormalization factor.

The reason why the above two approximations have been so successful for simple semiconductors[17,18] is that in these systems the self-energy shows a smooth linear behavior around the Fermi energy, and the quasiparticle and LDA wave functions are almost identical. Since the validity of these two approximations is not clear for correlated system such as VO_2, in this work we perform calculations without using these approximations; a frequency dependence of the self-energy is explicitly taken into account and the off-diagonal elements of the self-energy (in the Kohn-Sham basis) are included properly in the calculation. The quasiparticle energies are calculated by solving the following equation:

$$\det[(\omega-\varepsilon^{\mathrm{LDA}}_{\mathbf{k}\nu})\delta_{\mu\nu} - \Re\Delta\Sigma_{\mu\nu}(\mathbf{k},\omega)] = 0. \quad (5)$$

Here $\Re$ means the Hermitian part [i.e., $\Re A = \frac{1}{2}(A+A^\dagger)$]. When off-diagonal elements of $\Delta\Sigma(\mathbf{k},\omega)$ are not negligible, we calculate the roots of Eq. (5) by using the following linearization scheme: first we calculate $\Delta\Sigma(\mathbf{k},\omega)$ on a uniform frequency mesh $\omega_j = \omega_1 + \Delta\omega(j-1)$. In each region $\omega_j \le \omega \le \omega_{j+1}$, we linearly interpolate $\Delta\Sigma_{\mu\nu}(\mathbf{k},\omega)$ as

$$\Delta\Sigma_{\mu\nu}(\mathbf{k},\omega) = \frac{\omega_{j+1}-\omega}{\omega_{j+1}-\omega_j}\Delta\Sigma_{\mu\nu}(\mathbf{k},\omega_j) + \frac{\omega-\omega_j}{\omega_{j+1}-\omega_j}\Delta\Sigma_{\mu\nu}(\mathbf{k},\omega_{j+1}). \quad (6)$$

By substituting the above approximation for $\Delta\Sigma_{\mu\nu}(\mathbf{k},\omega)$ into Eq. (5), the roots of Eq. (5) are easily calculated by solving the generalized eigenvalue problem. We note that, unlike the usual linearization [Eq. (3)], this scheme is exact in the limit $\Delta\omega \to 0$.

Our calculation is based on the full-potential linear muffin-tin orbital (LMTO) basis.[19] The product-basis technique is used[20] and the frequency integral in Eq. (1) is numerically carried out along the imaginary axis including the contributions from the poles of the Green function.[21] Details of the GW code are described in Ref. 22. Vanadium $3s$ and $3p$ electrons are treated as valence electrons, and 151 unoccupied bands per V_2O_4 are used to compute G and W. To check the convergence of our calculations, we have also performed calculations with 100 unoccupied bands per V_2O_4 and found that the calculated band gaps in the insulating state differ only by about 0.01 eV. For the sampling of the Brillouin zone, $6\times6\times6$ ($4\times4\times4$) Monkhorst-Pack grid[23] is used for R (M_1) structure. In both phases, the experimental lattice parameters are used.[24,25]

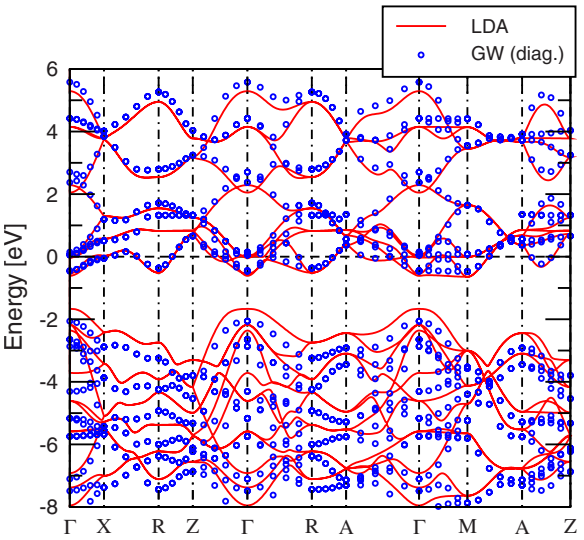

FIG. 1. (Color online) Band structure of metallic VO_2 calculated with the LDA (solid lines) and GW with only the diagonal self-energy (circles).

III. RESULTS AND DISCUSSION

A. Metallic tetragonal VO_2

Figure 1 shows the band structure of metallic VO_2 calculated within the LDA and the GWA. We find that the change

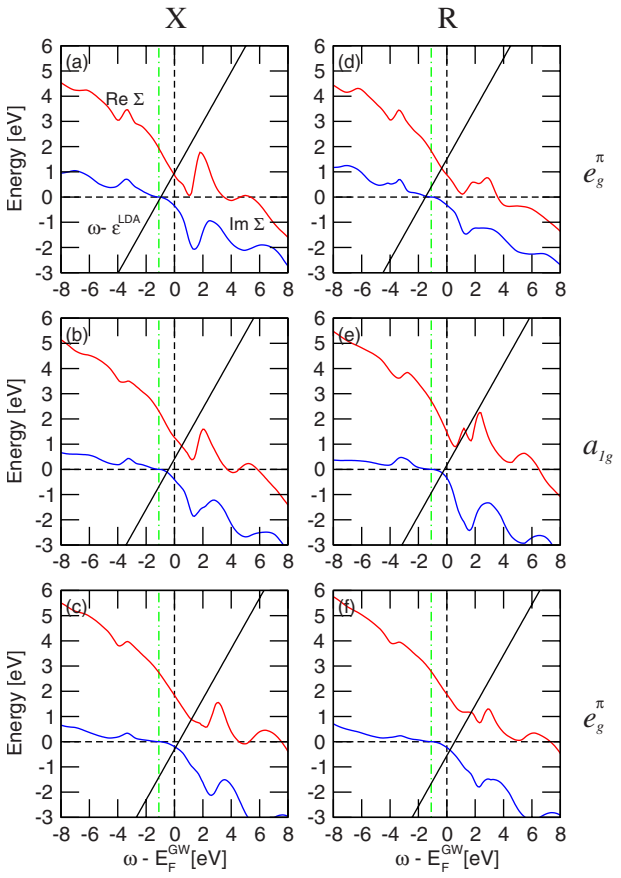

FIG. 2. (Color online) Diagonal self-energy $\Delta\Sigma_{\nu\nu}(\mathbf{k},\omega)$ for three t_{2g} bands of metallic VO_2 at the [(a)-(c)] X and [(d)-(f)] R points. In (b) and (e), the wave functions have mainly a_{1g} character, and in (a), (c), (d), and (f), the wave functions have mainly e_g^π character. Red lines: Re $\Delta\Sigma_{\nu\nu}(\mathbf{k},\omega)$. Blue lines: Im $\Delta\Sigma_{\nu\nu}(\mathbf{k},\omega)$. Black solid lines: $\omega-\varepsilon_{\mathbf{k}\nu}^{\mathrm{LDA}}$. The origin of the horizontal axes is set to the renormalized Fermi energy E_F^{GW} and E_F^{LDA} is shown as vertical dash-dotted lines.

in the quasiparticle energy due to the off-diagonal self-energy is negligible so that we consider only the diagonal self-energy. The broad oxygen $2p$ band lies from -8 to -2 eV, and a separation between the vanadium t_{2g} (which extends from -1 to 2 eV) and e_g bands (from 2 to 5 eV) is seen. This result is in agreement with previous calculations.[26] Compared to the LDA result, the self-energy correction makes the d-p separation larger by about 0.6 eV but the bandwidth of the d bands does not show a significant change. We find that, due to the dynamical correlation effects at some k points (not seen in Fig. 1), the number of roots of Eq. (5) becomes greater than the number of bands considered. In order to study the origin of this dynamical effect, we plot in Fig. 2 the frequency dependence of the diagonal self-energy $\Delta\Sigma_{\nu\nu}(\mathbf{k},\omega)$ for the t_{2g} bands at representative X and R points. When the off-diagonal self-energy is neglected, the roots of the quasiparticle equation [Eq. (5)] are given graphically by the intersections of two lines $\omega-\varepsilon_{\mathbf{k}\nu}^{\mathrm{LDA}}$ and Re $\Delta\Sigma_{\nu\nu}(\mathbf{k},\omega)$. For these bands a noticeable peak is found at around 2–3 eV in Re $\Delta\Sigma_{\nu\nu}(\mathbf{k},\omega)$, which produces the extra solutions of Eq. (5). Noting that in the GW approximation the imaginary part of the self-energy is related to W as[14]

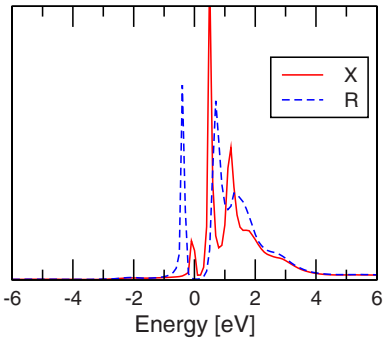

FIG. 3. (Color online) Spectral function $A(\mathbf{k},\omega)$ for t_{2g} bands of metallic VO_2 at the X (solid line) and R points (dashed line).

$$\mathrm{Im}\,\Sigma_{\nu\nu}^{c}(\mathbf{k},\omega>E_F)=-\sum_{\mathbf{q}}^{\mathrm{unocc}}\sum_{\mu}\sum_{\alpha\beta}\langle\psi_{\mathbf{k}\nu}\psi_{\mathbf{q}-\mathbf{k}\mu}|B_{\mathbf{q}\alpha}\rangle \times \mathrm{Im}\,W_{\alpha\beta}^{c}(\mathbf{q},\omega-\varepsilon_{\mathbf{q}-\mathbf{k}\mu}) \times\langle B_{\mathbf{q}\beta}|\psi_{\mathbf{q}-\mathbf{k}\mu}\psi_{\mathbf{k}\nu}\rangle\theta(\omega-\varepsilon_{\mathbf{q}-\mathbf{k}\mu}), \quad (7)$$

and

$$\mathrm{Im}\,\Sigma_{\nu\nu}^{c}(\mathbf{k},\omega\le E_F)=\sum_{\mathbf{q}}^{\mathrm{occ}}\sum_{\mu}\sum_{\alpha\beta}\langle\psi_{\mathbf{k}\nu}\psi_{\mathbf{q}-\mathbf{k}\mu}|B_{\mathbf{q}\alpha}\rangle \times \mathrm{Im}\,W_{\alpha\beta}^{c}(\mathbf{q},\varepsilon_{\mathbf{q}-\mathbf{k}\mu}-\omega) \times\langle B_{\mathbf{q}\beta}|\psi_{\mathbf{q}-\mathbf{k}\mu}\psi_{\mathbf{k}\nu}\rangle\theta(\varepsilon_{\mathbf{q}-\mathbf{k}\mu}-\omega), \quad (8)$$

where $\{B_{\mathbf{q}\alpha}\}$ is an arbitrary set of basis functions and the superscript c signifies the correlation part, this peak structure can be traced back to the corresponding peak in Im $W(\omega)$ or equivalently Im $\epsilon^{-1}(\omega)$, where $\epsilon(\omega)$ is the dielectric function. We actually find a strong peak in Im $\epsilon^{-1}(\omega)$ around 2 eV, which may be interpreted as a subplasmon arising from strong transitions from the narrow a_{1g} band to empty states just above the Fermi level. It is interesting to note that the peak in Im Σ above the Fermi level is much stronger than the peak below the Fermi level. This difference in the strength of the peaks most likely originates from the matrix elements, as can be clearly seen in the above expression for Im Σ.

In the metallic phase, the orbital dependence of the self-energy for these t_{2g} orbitals is small, which reflects the weak orbital polarization in this phase. We also find that the self-energy shows some k dependence; for the X point [Figs. 2(a)–2(c)] and other k points that lie on the plane $k_z=0$, where k_z is a reciprocal vector parallel to the c axis, the self-energy shows similar or "isotropic" behavior while for the R point [Figs. 2(d)–2(f)] and other k points that lie on $k_z=\frac{\pi}{c}$ plane, the self-energy is anisotropic and a peak around 2 eV is more pronounced for the a_{1g} [Fig. 2(e)] than for the e_g^π symmetry (Figs. 2(d) and 2(f)].

To see the consequence of the subplasmon peak, we plot the diagonal spectral function $A(\mathbf{k},\omega)=\sum_\nu\frac{1}{\pi}\left|\mathrm{Im}\frac{1}{\omega-\varepsilon_{\mathbf{k}\nu}^{\mathrm{LDA}}-\Delta\Sigma_{\nu\nu}(\mathbf{k},\omega)}\right|$ for the t_{2g} bands at X and R points in Fig. 3. Since the self-energy is calculated with the unshifted LDA Fermi energy, we shift the frequency dependence of Im Σ according to Im $\Sigma(\omega)\rightarrow$Im $\Sigma(\omega-\Delta E_F)$,

where $\Delta E_F = E_F^{GW} - E_F^{LDA}$, in order to reproduce the small inverse lifetime of the quasiparticles around the Fermi energy. Close to the Fermi energy, there are sharp quasiparticle peaks and the subplasmon-originated peak at around 2–3 eV in the self-energy yields a weak satellite structure. The renormalization factor $Z_{\mathbf{k}\nu}$ of the t_{2g} bands is about 0.5, which indicates a strong transfer of the spectral weight from the quasiparticle region to the incoherent part. In the DMFT calculation by Liebsch *et al.*[10] and the cluster-DMFT calculation by Biermann *et al.*,[12] the satellite structure is found also below the quasiparticle peak at around −1.5 eV, which is also observed in recent photoemission spectra.[2] That satellite, regarded as the lower Hubbard band, is not seen in our calculation.

The self-energy of the real system differs from that of the Hubbard model in the following fashion. The energy scale of the self-energy of the Hubbard model is determined by U, which is of the order of a few eV, whereas the energy scale of the self-energy of the real system is determined by the bare Coulomb interaction, which is typically one order of magnitude larger than the Hubbard U. As a result, Im Σ of the Hubbard model decays to zero after a few eV, above and below the Fermi level, whereas Im Σ of the real system decays to zero at energies larger than the plasmon energy, which is of the order of tens of eV. As can be seen in Fig. 2 the presence of high-energy plasmon excitation causes Im Σ to increase to a large value outside the energy range of approximately −4 and 4 eV, in contrast to the Hubbard model in which Im Σ decays to zero outside this energy range. The decay of Im Σ enhances the satellite structure and may actually overemphasize the strength of the satellite, as discussed in Ref. 27. Nevertheless, experimentally there appears to be some evidence that there exists indeed a satellite structure a few eV below the Fermi level.[2] In order to reproduce that peak, one must include short-range correlation effects beyond the RPA; for this purpose it would be very interesting to apply methods such as GW+DMFT (Ref. 28) to this system.

B. Insulating monoclinic VO_2

Figure 4 shows the band structure of the insulating monoclinic VO_2 calculated within the LDA and the GWA with only the diagonal part of the self-energy. As in the metallic phase, we see the separation of the t_{2g} and e_g bands due to the octahedral crystal field, and the downward shift of O $2p$ bands. However, in this phase the occupied part of V $3d$ states is mainly of a_{1g} character, which results from the pairing of the vanadium atoms. To evaluate the effects of the off-diagonal self-energy on the band structure, we compare the results with and without the off-diagonal self-energy in Fig. 5. In this calculation the matrix elements of the self-energy are calculated within the V d subspace. We find that inclusion of the O $2p$ bands changes the quasiparticle energies by less than 0.1 eV. In most bands the off-diagonal self-energy is very small and the two results are almost the same but a noticeable difference is found near the Fermi energy. In the diagonal-only GW result [Fig. 5(b)], an unusual band overlap around point A is found, which is removed when the off-diagonal self-energy is included. This anomaly is attributed to the inefficiency of both the LDA and the one-shot GWA. Around point A, the valence (a_{1g}) and conduction (e_g^{π}) bands are barely separated at the LDA level [Fig. 5(a)] so these bands are "fictitiously" hybridized. Since the diagonal-only GW calculation does not change the character of the wave functions, this hybridization cannot be removed unless the off-diagonal self-energy is included. Thus, the LDA wave functions and the quasiparticle ones obtained by including the off-diagonal self-energy are far from identical.

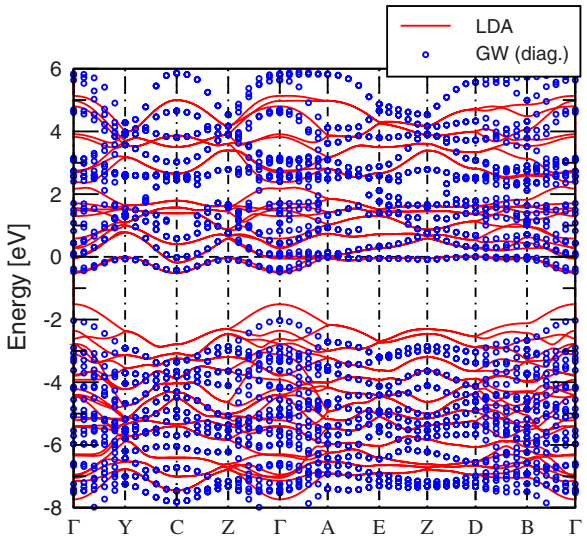

FIG. 4. (Color online) Band structure of insulating VO_2 calculated with the LDA (solid lines) and GW including only a diagonal part of the self-energy (circles). The symmetry labels are the same as those in Ref. 26.

At first sight the presence of bands crossing the Fermi level at around point A intuitively suggests that it is unlikely to open up a gap around that point. In the case of a single band crossing the Fermi level, there appears to be no choice other than an opening of a Mott gap. However, in the case of VO_2, there are multibands, which still allow for an opening of a gap within a one-particle picture by means of rearrangement of the band occupation. This is indeed the case and it is noteworthy that the rearrangement of the band occupation around point A is already obtained in the one-shot GW calculation, provided the off-diagonal self-energy is taken into account.

We thus observe two important ingredients in gap opening in narrow-band materials where entangled bands cross the Fermi level: First, the off-diagonal self-energy is crucial in "dehybridizing" the bands and rearranging the band occupation, and second, the modification of the one-particle energies decreases the screening and hence enhances the gap opening[29,30] in the course of self-consistency. This is in contrast to the conventional semiconductors where the gap opening, in the case of overlapping valence and conduction bands, is simply affected by shifting the bands, i.e., by the second mechanism.

We also find that due to the nonlinear behavior of the self-energy, it is crucial to take into account the frequency

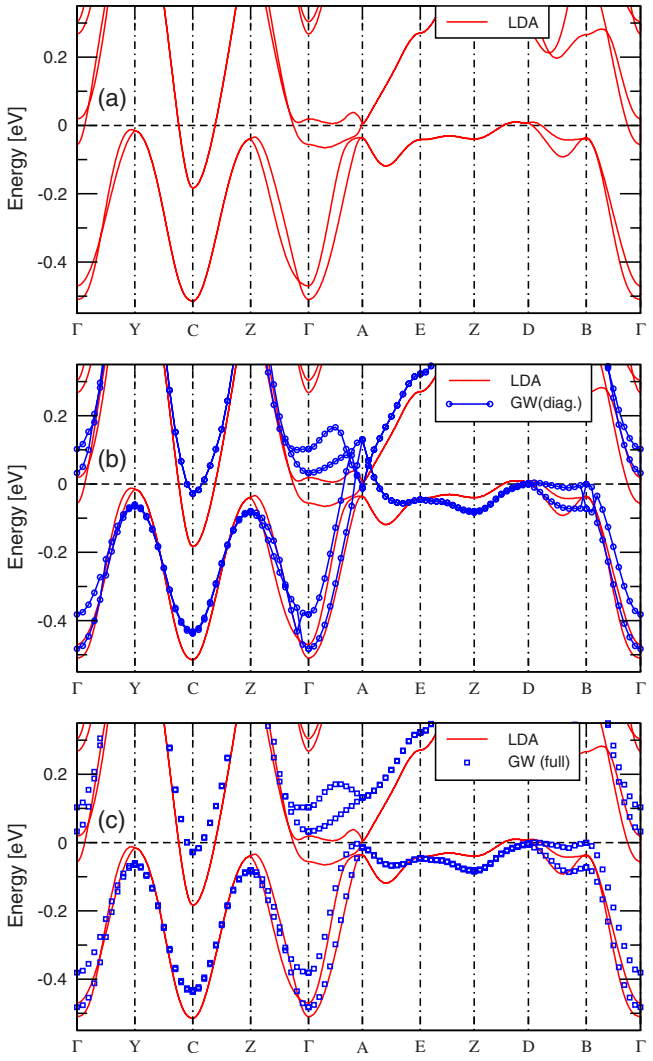

FIG. 5. (Color online) Band structure of insulating VO_2 near the Fermi energy calculated with (a) LDA and (b) GW including only a diagonal part of the self-energy, and (c) GW including the off-diagonal self-energy.

dependence of the self-energy explicitly in calculating $\{\varepsilon^{\mathrm{GW}}_{\mathbf{k}\nu}\}$. The results with and without the linearization are compared in Fig. 6. The usual linearized approach [Eq. (4)], which is used in most one-shot GW calculations, causes an error of as much as 0.2 eV for the a_{1g} band, which leads to underestimation of the valence bandwidth and hence overestimation of the band gap. Figures 7(a)–7(c) show the diagonal self-energy for the insulating phase at Γ and E for three bands: bonding and antibonding a_{1g} and e_g^{π}. The self-energy for other k points shows a similar behavior. A nonlinear behavior of the self-energy is clearly seen from the figure, which explains the failure of the usual linearization scheme. Owing to the lattice distortion, the self-energy for these t_{2g} bands shows strong orbital dependence, in contrast to the metallic phase; peak structures in Re Σ around −4 and 1–3 eV arising from strong transition from the narrow a_{1g} band to empty states just above the Fermi level are more prominent for a_{1g} bands. This peak yields extra solutions to Eq. (5), which are seen as flat bands around 2.5 eV in Fig. 4. The renormalization factor for these bands is about 0.5–0.6.

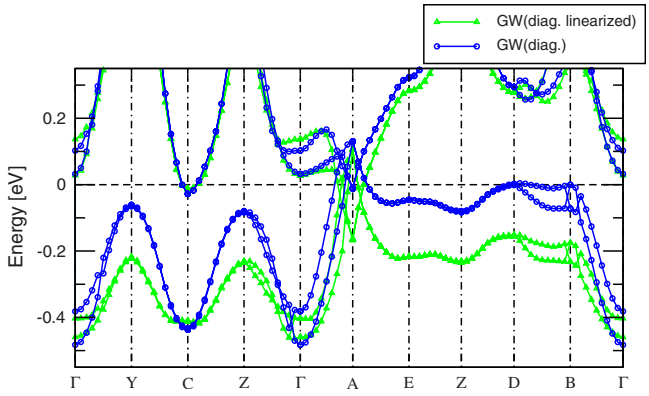

FIG. 6. (Color online) GW band structure of insulating VO_2. Triangles (circles) correspond to the result with (without) the linearization of the self-energy. Only the diagonal self-energy is included in the calculation.

In our one-shot GW result, even if the off-diagonal self-energy is included, there still exists a small indirect band overlap of 0.02 eV in contrast to the experimental band gap

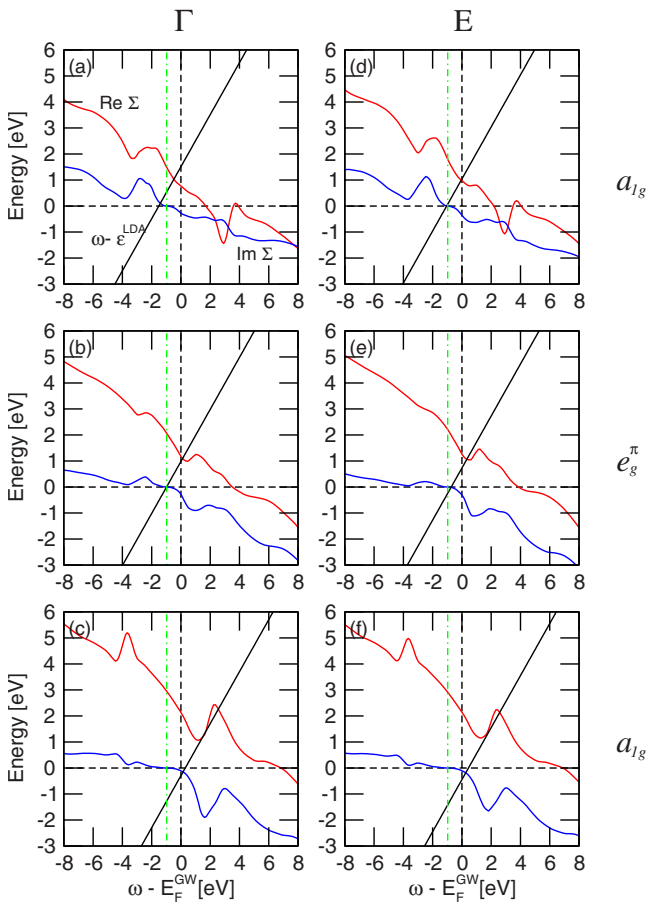

FIG. 7. (Color online) Diagonal self-energy $\Delta\Sigma_{\nu\nu}(\mathbf{k},\omega)$ of insulating VO_2 for t_{2g} bands in the one-shot GW calculation at the [(a)-(c)] Γ and [(d)-(f)] E points. (a) and (d): bonding a_{1g} bands. (b) and (e): e_g^{π} bands. (c) and (f): antibonding a_{1g} bands. Red lines: $\mathrm{Re}\Delta\Sigma_{\nu\nu}(\mathbf{k},\omega)$. Blue lines: $\mathrm{Im}\,\Delta\Sigma_{\nu\nu}(\mathbf{k},\omega)$. Black solid lines: $\omega - \varepsilon^{\mathrm{LDA}}_{\mathbf{k}\nu}$. The origin of the horizontal axes is set to the renormalized Fermi energy E_F^{GW} and E_F^{LDA} is shown as vertical dash-dotted lines.

of 0.6 eV. Furthermore, the bonding-antibonding splitting of a_{1g} bands is less than 2 eV, noticeably smaller than the experiment.[2] The present calculation uses the LDA wave functions and eigenenergies to construct G and W. Thus, the failure to reproduce the experimental gap may be due to the poorness of the starting states and a calculation starting from a better mean-field solution will be needed to test the initial-state dependence. Indeed, very recently Gatti *et al.* attempted such a calculation.[16] They first performed a static COHSEX calculation self-consistently and obtained an insulating phase. The result was used as the starting Hamiltonian of a subsequent one-shot GW calculation, which yielded a final band gap in good agreement with experiment. They found that, without modification of the LDA wave functions, the gap was not opened.

Since a self-consistent GW scheme[22,31–34] is not yet well established,[35,36] it would be meaningful to study the effect of initial states[37] and self-consistency. The problem is how to construct a one-particle Hamiltonian whose eigenfunctions and energies well represent the quasiparticle wave functions and energies. One possible way is a so-called quasiparticle self-consistent scheme (QSGW) proposed in Ref. 38 where the exchange and correlation part of the one-particle Hamiltonian is replaced by a static nonlocal exchange-correlation potential constructed using the following formula:

$$\langle \psi^{\mathrm{LDA}}_{\mathbf{k}\mu} | \hat{v}_{xc} | \psi^{\mathrm{LDA}}_{\mathbf{k}\nu} \rangle = \frac{\Re}{2} [\Sigma_{\mu\nu}(\mathbf{k}, \varepsilon^{\mathrm{GW}}_{\mathbf{k}\mu}) + \Sigma_{\nu\mu}(\mathbf{k}, \varepsilon^{\mathrm{GW}}_{\mathbf{k}\nu})], \quad (9)$$

with the self-energy Σ calculated in the GWA. The reason for introducing such a recipe is that the self-energy is energy dependent. For the diagonal elements ($\mu = \nu$), no ambiguities arise in choosing the energy but for the off-diagonal elements, the choice of the energy is ambiguous. The formula, however, still awaits theoretical justification.

As another choice, we propose the following procedure. The quasiparticle wave functions $\{\Psi_{\mathbf{k}\nu}\}$, obtained as solutions of Eq. (2) with Im Σ neglected, are in general not orthogonal and therefore unsuitable as an input for a GW calculation. We envisage that a natural and physically motivated quasiparticle Hamiltonian is

$$H_{\mathrm{QP}} = \sum_{\mathbf{k}\nu} |\Psi_{\mathbf{k}\nu}\rangle \varepsilon^{\mathrm{GW}}_{\mathbf{k}\nu} \langle \Psi_{\mathbf{k}\nu}|, \quad (10)$$

which may be viewed as a series of quasiparticle modes (QPM). This quasiparticle Hamiltonian is evidently Hermitian and ambiguities in choosing the energy in the self-energy do not arise. Upon diagonalizing H_{QP}, we obtain an orthonormal set of wave functions with the corresponding eigenvalues. In most cases the quasiparticle wave functions are almost orthogonal; thus the solutions of Eq. (10) should be very close to the original quasiparticle states.

To convince ourselves that our QPM approximation is physically sound, we compare in Fig. 8 the quasiparticle band structures generated from the solutions of Eq. (5) and the QPM approximation [Eq. (10)], as well as the QSGW [Eq. (9)]. In this calculation, the self-energy Σ is calculated with LDA eigenstates (i.e., non-self-consistent calculation). As can be seen, the QPM band structure agree with the true

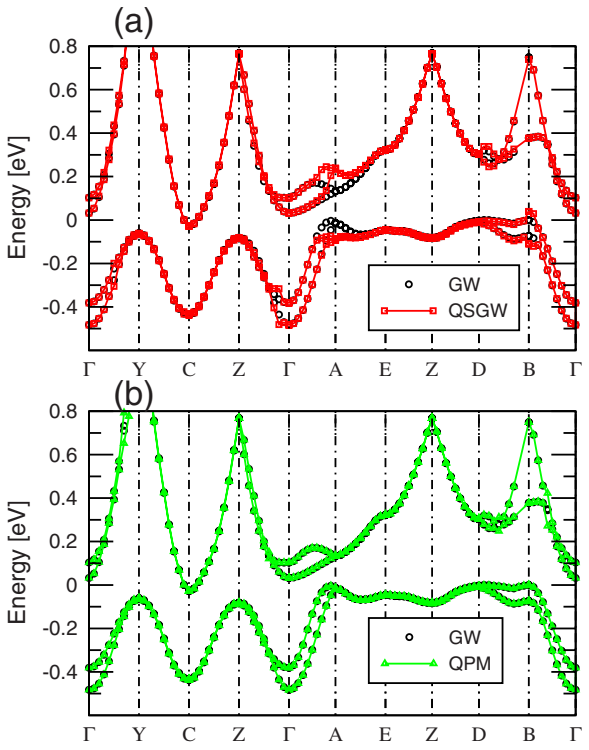

FIG. 8. (Color online) Band structure of insulating VO_2 calculated with (a) GW (circles) and QSCW (squares), and (b) GW (circles) and QPM (triangles).

quasiparticle band structure well within the accuracy of the calculations whereas the band structure calculated using Eq. (9) shows a noticeable deviation from the true quasiparticle band structure around point A. This deviation originates from the approximated form of the off-diagonal part of the effective exchange-correlation potential. Thus, the quasiparticle energy can be sensitive to the choice of the energy in the self-energy. On the other hand, the QPM approximation is free from ambiguity in choosing the energy argument in the self-energy and the off-diagonal self-energy is properly taken into account implicitly via the quasiparticle wave function [Eq. (10)].

A self-consistent scheme is now at our disposal. We start by performing a GW calculation using the LDA band structure as an input. The resulting self-energy is then used to construct the quasiparticle wave functions and energies by solving Eq. (5). A set of wave functions and energies are obtained within the QPM approximation in Eq. (10), and used to perform the next GW calculation. The iteration continues until the quasiparticle wave functions and energies converge. For the case of VO_2 that we are considering, this is a very cumbersome task due to the large system size. We have observed, however, the following result: starting from the metallic LDA band structure, the quasiparticle band structure obtained by solving Eq. (5) acquires a (direct) gap already in the first iteration. This suggests that the rearrangement of the wave functions already takes place in the first iteration and, after the first iteration of the present method, we may then keep the same wave functions. The self-energy is assumed to be diagonal except within the V d subspace. It is important to note that the gap around point A is not opened

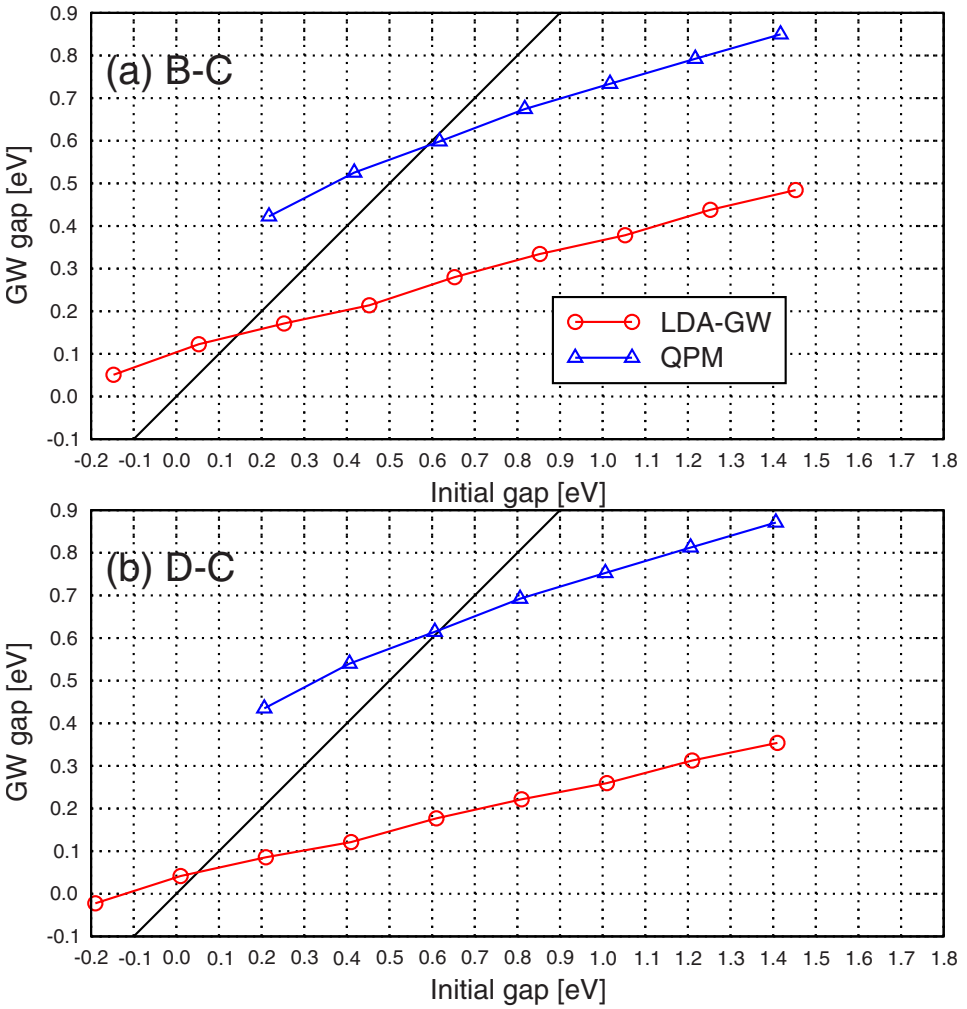

FIG. 9. (Color online) GW indirect gap between (a) B and C, and (b) D and C as a function of the initial band gap with the self-energy calculated by using the wave functions obtained within the LDA (circles) and QPM (triangles).

up if the off-diagonal elements of the self-energy within the t_{2g} subspace are not taken into account. In the subsequent iterations, we simulate the self-consistency by uniformly shifting the conduction-band quasiparticle energies according to $E_{\mathbf{k}c} \rightarrow E_{\mathbf{k}c} + \Delta$. The self-consistent solution is defined as the point where the input gap and the calculated gap match. We have tested this simplified self-consistent scheme for simple semiconductors and found that it yields a result very close to that of the full QPM self-consistent calculation. In the actual calculation of VO_2, we start the calculation from a state with a gap, obtained by adding an initial shift of Δ_0 to the LDA conduction levels. In our simplified procedure, this process is necessary to simulate the insulating state in constructing the self-energy matrix because the LDA yields a metallic state. This initial shift is not needed if we perform a truly self-consistent calculation. In the first iteration we calculate the self-energy and quasiparticle states [from Eq. (5)] by using the LDA states with the initial shift of Δ_0 to construct one-particle wave functions and eigenenergies via Eq. (10), and use these states as an input for our simplified self-consistent calculation; we search for the self-consistent solution by recalculating the self-energy and band gap with the new wave functions and energies where the conduction-band energies are uniformly shifted by Δ, and plotting the output gap as a function of the input gap. We have performed calculations with several choices of Δ_0 (from 0.4 to 1.2 eV) and found that the self-consistent solution is not sensitive to the value of the initial shift Δ_0 as long as it is large enough to open a gap.

The result of the gaps as a function of the shift is shown in Fig. 9. Two indirect gaps are shown, one between points B and C, and the other between D and C. The GW gaps increase almost linearly with the shift and a self-consistent value of 0.6 eV is found within the QPM approximation. This result differs considerably from the result obtained by assuming that the self-energy is diagonal, i.e., the wave functions are given by those of the LDA. Our results show that the GWA within the quasiparticle concept is sensitive to the treatment of the off-diagonal elements of the self-energy, which modify the LDA wave functions. Although a proper definition of an effective quasiparticle Hamiltonian is debatable,[16,34,38] the obtained 0.6 eV gap in our calculation, which happens to be in good agreement with the experimental value, is an indication that our QPM scheme could furnish a suitable way of constructing a quasiparticle Hamiltonian.

Our result makes us reconsider the electronic state of the paramagnetic insulating VO_2; in the Peierls description, the bonding-antibonding separation of the a_{1g} bands is determined only by the hybridization between the two a_{1g} bands, and both spin-up and spin-down states are assumed to occupy the same (bonding a_{1g}) orbitals. However, the Coulomb interaction between localized d electrons would seem to in-

validate this interpretation, as is clear from the example of a two-site Hubbard model. Thus, the paramagnetic insulating VO_2 may be the result of a singlet state formed by two localized electrons on paired vanadium atoms.[12] However, it is shown in Ref. 12 that a one-particle description can also provide a good description of the quasiparticle band structure. Our result along with previous calculations[15,16] also suggest that a one-particle description can still go a long way in describing the electronic structure of VO_2, at least in describing the insulating gap. Nevertheless, we think that the Peierls picture alone may not be sufficient for a complete description of the electronic structure of the insulating VO_2. The missing satellite below the Fermi level, observed in photoemission experiment, is one such indication.

IV. CONCLUSION

In conclusion, we have investigated the self-energy and band structure of the metallic and insulating phases of VO_2 within the GWA. In agreement with the work of Gatti *et al.*, we have found that the GWA is able to describe the metal-insulator transition. Our calculations indicate that the band gap depends sensitively on the approximation used for the off-diagonal elements of the self-energy. Thus, a proper way of defining the off-diagonal elements of the self-energy is crucial. Using the QPM approximation and the scissor operator, we have performed a self-consistent calculation to determine the band gap, which is found to be 0.6 eV, in agreement with calculated value by Gatti *et al.* albeit using different methods. Our results within the QPM approximation suggest that the GWA can treat correlation effects in VO_2 and the opening of the gap supports the Peierls picture of Wentzcovitch *et al.* It does not seem to be necessary to perform calculations with broken spin symmetry (antiferromagnetic structure) as commonly done in order to open up a gap.[39]

In both the metallic and insulating phases, a satellite feature exists above the Fermi energy but not below, in contrast to the spectra calculated within the LDA+DMFT scheme. Since the experimental photoemission spectrum displays satellite features above and below the Fermi level, usually interpreted as the upper and lower Hubbard bands, we attribute the discrepancy of the GW spectra to vertex corrections, i.e., correlations beyond the RPA, which are apparently captured in the LDA+DMFT.

We have also found that the common procedure of calculating the quasiparticle energy by linearization of the self-energy fails badly in the case of VO_2. It would seem that for narrow-band materials it is important to take into account the full energy dependence of the self-energy when calculating the quasiparticle energy.

ACKNOWLEDGMENTS

We thank S. Biermann, J. Tomczak, L. Reining, and M. Gatti for fruitful discussions. We also acknowledge the use of the full-potential LMTO-GW code provided to us by T. Kotani and M. van Schilfgaarde. This work was supported by Grant-in-Aid for Scientific Research from MEXT, Japan (Grants No. 19019013 and No. 19051016).

*reis@faculty.chiba-u.jp

[1] J. Morin, Phys. Rev. Lett. **3**, 34 (1959).
[2] T. C. Koethe, Z. Hu, M. W. Haverkort, C. Schüßler-Langeheine, F. Venturini, N. B. Brookes, O. Tjernberg, W. Reichelt, H. H. Hsieh, H.-J. Lin, C. T. Chen, and L. H. Tjeng, Phys. Rev. Lett. **97**, 116402 (2006).
[3] J. B. Goodenough, J. Solid State Chem. **3**, 490 (1971).
[4] R. M. Wentzcovitch, W. W. Schulz, and P. B. Allen, Phys. Rev. Lett. **72**, 3389 (1994).
[5] J. P. Pouget, H. Launois, T. M. Rice, P. Dernier, A. Gossard, G. Villeneuve, and P. Hagenmuller, Phys. Rev. B **10**, 1801 (1974).
[6] J. P. Pouget, H. Launois, J. P. D'Haenens, P. Merender, and T. M. Rice, Phys. Rev. Lett. **35**, 873 (1975).
[7] A. Zylbersztejn and N. F. Mott, Phys. Rev. B **11**, 4383 (1975).
[8] T. M. Rice, H. Launois, and J. P. Pouget, Phys. Rev. Lett. **73**, 3042 (1994).
[9] A. Georges, G. Kotliar, W. Krauth, and M. J. Rozenberg, Rev. Mod. Phys. **68**, 13 (1996).
[10] A. Liebsch, H. Ishida, and G. Bihlmayer, Phys. Rev. B **71**, 085109 (2005).
[11] M. S. Laad, L. Craco, and E. Müller-Hartmann, Phys. Rev. B **73**, 195120 (2006).
[12] S. Biermann, A. Poteryaev, A. I. Lichtenstein, and A. Georges, Phys. Rev. Lett. **94**, 026404 (2005).
[13] L. Hedin, Phys. Rev. **139**, A796 (1965).
[14] F. Aryasetiawan and O. Gunnarsson, Rep. Prog. Phys. **61**, 237 (1998).
[15] A. Continenza, S. Massidda, and M. Posternak, Phys. Rev. B **60**, 15699 (1999).
[16] M. Gatti, F. Bruneval, V. Olevano, and L. Reining, Phys. Rev. Lett. **99**, 266402 (2007).
[17] M. S. Hybertsen and S. G. Louie, Phys. Rev. B **34**, 5390 (1986).
[18] R. W. Godby, M. Schlüter, and L. J. Sham, Phys. Rev. B **37**, 10159 (1988).
[19] M. Methfessel, M. van Schilfgaarde, and R. A. Casali, in *Electronic Structure and Physical Properties of Solids: The Uses of the LMTO Method*, edited by H. Dreysse, Lecture Notes in Physics Vol. 535 (Springer-Verlag, Berlin, 2000).
[20] F. Aryasetiawan and O. Gunnarsson, Phys. Rev. B **49**, 16214 (1994).
[21] F. Aryasetiawan, in *Strong Coulomb Correlations in Electronic Structure Calculations*, edited by V. I. Anisimov (Gordon and Breach, Singapore, 2000).
[22] T. Kotani, M. van Schilfgaarde, and S. V. Faleev, Phys. Rev. B **76**, 165106 (2007).
[23] H. J. Monkhorst and J. D. Pack, Phys. Rev. B **13**, 5188 (1976).
[24] D. B. McWhan, M. Marezio, J. P. Remeika, and P. D. Dernier, Phys. Rev. B **10**, 490 (1974).
[25] J. M. Longo and P. Kierkegaard, Acta Chem. Scand. (1947-

1973) **24**, 420 (1970).
[26] V. Eyert, Ann. Phys. **11**, 9 (2002).
[27] F. Aryasetiawan, M. Imada, A. Georges, G. Kotliar, S. Biermann, and A. I. Lichtenstein, Phys. Rev. B **70**, 195104 (2004).
[28] S. Biermann, F. Aryasetiawan, and A. Georges, Phys. Rev. Lett. **90**, 086402 (2003).
[29] T. Miyake, F. Aryasetiawan, H. Kino, and K. Terakura, Phys. Rev. B **61**, 16491 (2000).
[30] R. Sakuma, T. Miyake, T. Kotani, M. van Schilfgaarde, and S. Tsuneyuki (unpublished).
[31] B. Holm and U. von Barth, Phys. Rev. B **57**, 2108 (1998).
[32] W. Ku and A. G. Eguiluz, Phys. Rev. Lett. **89**, 126401 (2002).
[33] F. Bruneval, N. Vast, and L. Reining, Phys. Rev. B **74**, 045102 (2006).
[34] M. Shishkin, M. Marsman, and G. Kresse, Phys. Rev. Lett. **99**, 246403 (2007).
[35] K. Delaney, P. Garcia-Gonzalez, A. Rubio, P. Rinke, and R. W. Godby, Phys. Rev. Lett. **93**, 249701 (2004).
[36] W. Ku and A. G. Eguiluz, Phys. Rev. Lett. **93**, 249702 (2004).
[37] T. Miyake, P. Zhang, M. L. Cohen, and S. G. Louie, Phys. Rev. B **74**, 245213 (2006).
[38] S. V. Faleev, M. van Schilfgaarde, and T. Kotani, Phys. Rev. Lett. **93**, 126406 (2004).
[39] M. A. Korotin, N. A. Skorikov, and V. I. Anisimov, Phys. Met. Metallogr. **94**, 17 (2002).